Journal of Chromatography A, 1218 (2011) 2203–2213

Contents lists available at ScienceDirect

Journal of Chromatography A

journal homepage: www.elsevier.com/locate/chroma

Mobile phase effects in reversed-phase liquid chromatography: A comparison of acetonitrile/water and methanol/water solvents as studied by molecular simulation

Jake L. Rafferty [a], J. Ilja Siepmann [a,b,*], Mark R. Schure [c]

[a] Department of Chemistry, University of Minnesota, 207 Pleasant Street SE, Minneapolis, MN 55455-0431, USA
[b] Department of Chemical Engineering and Materials Science, University of Minnesota, 421 Washington Avenue SE, Minneapolis, MN 55455-0132, USA
[c] Theoretical Separation Science Laboratory, The Dow Chemical Company, 727 Norristown Road, Box 0904, Spring House, PA 19477-0904, USA

ARTICLE INFO

Article history:
Received 4 November 2010
Received in revised form 28 January 2011
Accepted 5 February 2011
Available online 15 February 2011

Keywords:
Reversed-phase liquid chromatography
Simulation
Retention mechanism
Stationary phase structure
Organic modifier
Acetonitrile
Methanol

ABSTRACT

Molecular simulations of water/acetonitrile and water/methanol mobile phases in contact with a C_{18} stationary phase were carried out to examine the molecular-level effects of mobile phase composition on structure and retention in reversed-phase liquid chromatography. The simulations indicate that increases in the fraction of organic modifier increase the amount of solvent penetration into the stationary phase and that this intercalated solvent increases chain alignment. This effect is slightly more apparent for acetonitrile containing solvents. The retention mechanism of alkane solutes showed contributions from both partitioning and adsorption. Despite changes in chain structure and solvation, the molecular mechanism of retention for alkane solutes was not affected by solvent composition. The mechanism of retention for alcohol solutes was primarily adsorption at the interface between the mobile and stationary phase, but there were also contributions from interactions with surface silanols. The interaction between the solute and surface silanols become very important at high concentrations of acetonitrile.

1. Introduction

Reversed-phase liquid chromatography (RPLC) is among the most popular methods for the separation and analysis of chemical mixtures. Despite this popularity and decades of research, the complex interplay between solvent, stationary phase and solute that enacts a separation in RPLC is not fully understood. Retention in RPLC is driven by the distribution of solute molecules between the mobile phase (an aqueous/organic mixture) and the stationary phase (typically C_{18} alkyl chains tethered to silica surface). However, the molecular-level events that drive this distribution, or the retention mechanism, have been a topic of study for over 30 years and the key details are still not settled [1–26]. For example, there are conflicting views as to whether adsorption at the stationary phase/mobile phase interface or full partitioning into the stationary phase is more important for solute retention and to what extent various chromatographic parameters, such as mobile phase composition and grafting density, affect this mechanism [14,18,21,26]. Even if partitioning is taken to be the dominant mechanism of retention, it is not clear if the process can be modeled accurately by bulk liquid–liquid (e.g., oil–water) partitioning [14,23] or if partitioning into the tethered hydrocarbon chains of the RPLC stationary phase involves a different molecular mechanism [16,22]. Furthermore, it is debated whether the thermodynamic driving forces for solute retention (transfer from mobile to stationary phase) are primarily solvophobic [21] or lipophilic [14,23]. Here, solvophobic refers to the unfavorable interaction that an analyte molecule experiences with the polar mobile phase and lipophilic refers to favorable interaction with the nonpolar stationary phase.

The problem of pinpointing the retention mechanism in RPLC is further exacerbated by an incomplete understanding of the interaction between the mobile phase and the stationary phase. It is generally held that the organic component of the aqueous/organic mobile phase preferentially solvates the stationary phase. However, it is not fully resolved if this excess solvation occurs mainly through the formation of an organic layer atop the stationary phase [27,28] or if penetration of the organic modifier into the stationary phase is also important [29,30]. In the former case, retention could be affected by partitioning of the solutes into this organic layer, and in the latter case, solutes may compete with solvent molecules for space inside the stationary phase. In addition, changes in the level of solvation of the stationary phase with changing mobile phase composition may effect the conformation of the alkyl chains and alter their retentive properties.

* Corresponding author. Tel.: +1 612 624 1844.
E-mail address: siepmann@umn.edu (J.I. Siepmann).

0021-9673/$ – see front matter © 2011 Elsevier B.V. All rights reserved.
doi:10.1016/j.chroma.2011.02.012

For a true understanding of structure and retention in RPLC, molecular-level information is needed. However, it is often very difficult to attain these molecular details through experiments alone. For this reason, molecular simulation, which can provide these details directly, has been employed by numerous groups and has become an increasingly popular means for studying RPLC [31–59]. A critical aspect of simulating RPLC is the ability of the simulation technique to reproduce experimental retention data. If the simulation is unable to accurately generate these data, then it is difficult to have confidence in the corresponding molecular details. Our recent studies have shown that molecular simulations using efficient sampling algorithms and accurate force fields can yield high precision retention data that are in quantitative agreement with experiment [52,53,55–59]. Although much useful and interesting data have come from the simulations carried out by other groups [31,32,34–47,49], a demonstrated ability to accurately and precisely model solute retention has been lacking in these studies.

In a continuing effort by us to systematically discern the molecular-level effects of various chromatographic parameters on structure and retention in RPLC, the influences of methanol concentration in the mobile phase [52], alkyl chain length [56], grafting density [54,55,59], polar-embedded groups [53,56], pressure [56], and pore shape [56] have been examined. In the present work the effect of two organic modifiers at various concentrations is examined by carrying out simulations for a medium-coverage dimethyl octadecylsilane stationary phase in contact with various water/acetonitrile and water/methanol mixtures.

The effect of organic modifier concentration is an important topic because selectivity in RPLC is most often optimized by adjusting the composition of the mobile phase. In addition to the concentration, the identity of the organic modifier is also important. It has been suggested that the mechanism of retention can be altered when different organic modifiers are used. For example, the retention mechanism is thought to be more adsorption-like for water/acetonitrile and more partition-like for water/methanol mixtures [25]. Furthermore, the thermodynamics of the retention process are different depending on whether water/methanol or water/acetonitrile is used [23,60–63]. It is thought this may result from acetonitrile's greater affinity to aggregate around the solutes as compared to methanol [60–62] or that acetonitrile penetrates the stationary phase to a larger extent than methanol [63].

2. Simulation details

The simulation methodology used in this work closely follows our previous work [52–57]. Thus, only the salient features are described in this sections and the reader is referred to [57] for a very detailed description. To examine the effects of mobile phase composition in RPLC we make use of coupled–decoupled configurational-bias Monte Carlo simulations (CBMC) [64–68] in the isobaric–isothermal version of the Gibbs ensemble [69,70]. The simulations are carried out at a temperature of 323 K and a pressure of 1 atm and make use of three separate simulation boxes that are in thermodynamic contact but do not share an explicit interface (a graphical representation of the three-box set-up can be found in [54]). The first simulation box corresponds to a planar slit pore with two substrates, (1 1 1) surfaces of β-cristobalite separated by about 70 Å along the z-direction, to which dimethyl octadecylsilane chains are grafted at a density of 2.9 μmol/m^2 resulting in a residual silanol density of 4.8 μmol/m^2. The remainder of this pore is filled by mobile phase solvent. The second box contains a bulk mobile phase reservoir and the third box a helium vapor phase. These boxes are cubic and their volumes are allowed to fluctuate in response to the external pressure. In these Gibbs ensemble simulations, solvent and solute molecules are allowed to move between the three boxes, thereby ensuring that the chemical potentials of solvent species and analyte compounds are equal in the stationary phase box, the bulk solvent reservoir, and the vapor phase.

The vapor box present in these simulation serves as an ideal gas reference state, which allows one to decompose the free energy of retention into mobile and stationary phase components (ΔG_{mob} and ΔG_{stat}, respectively) [57,58].

Seven different aqueous/organic mobile phase compositions are compared: pure water, 33% molfraction acetonitrile, 67% molfraction acetonitrile, pure acetonitrile, 33% molfraction methanol, 67% molfraction methanol, and pure methanol (hereafter referred to as systems WAT, 33A, 67A, ACN, 33M, 67M, and MET, respectively). The data for systems WAT, 33M, 67M, and MET are taken from [51] and [52]. Each system contained from 768 to 1200 solvent molecules and 16 solutes (two each of C_1 to C_4 normal alkanes and alcohols).

To describe molecular interactions in the model RPLC system, the TraPPE force field [67,71–74] was used for alkanes, alcohols, acetonitrile, and helium. Water was described by the TIP4P model [75] and silica by a rigid zeolite potential [76–78]. Surface silanols were given bending and torsional degrees of freedom and had charges assigned based on the TraPPE alcohol model ($-0.739e$ for oxygen, $+0.435e$ for hydrogen) [72]. Lennard-Jones interactions were truncated at a distance of 10 Å and Coulombic interactions were treated with the Ewald summation technique [79] using a direct space cutoff of 10 Å and a convergence parameter of κ = 0.28. The number of reciprocal space vectors used in each direction of a box was equal to the next integer greater than $\kappa \times L_\alpha$, where L_α is the box length in that direction. It should be noted here that structural features and solvation thermodynamics can be very sensitive to the details of the molecular models (i.e., the underlying force fields). For example, relatively small changes in the partial charges and Lennard-Jones parameters used for acetonitrile were found to significantly alter the degree of microheterogeneity in water/acetonitrile mixtures [80]. Similarly, small changes in only the Lennard-Jones parameters of the alkyl tail were found responsible for large changes in water solubility, structure, and solute partitioning for octanol–water liquid–liquid equilibria [81,82]. Thus, with respect to computational investigations of retention mechanisms, it is of utmost importance to validate predicted retention data against experimental values.

For each solvent composition studied, four independent simulations were carried out. Each simulation was equilibrated for 2×10^5 Monte Carlo (MC) cycles (one MC cycle corresponds to N MC moves, where N is the total number of molecules in the system). Thereafter, the simulations proceeded with an additional 2×10^5 MC cycles during which averages were collected. Statistical uncertainties in all reported quantities were estimated from the standard error of the mean of the averages from the four independent simulations.

3. Results and discussion

Snapshots from the simulations at each solvent composition are shown in Fig. 1. Although each of these snapshots represents only a single configuration of the millions generated during the simulation, they already demonstrate some of the distinct differences between the seven solvent systems. As the fraction of organic modifier is increased, there is significantly more penetration of solvent into the stationary phase. Near the silica surface, most of this solvent is water. However, throughout the remainder of the stationary phase the majority of the sorbed solvent appears to be the organic modifier. In comparing systems with the same fraction of organic modifier, more solvent penetration is observed for the acetonitrile containing systems. Also appearing enriched in organic component of the solvent is the interfacial region between the stationary and

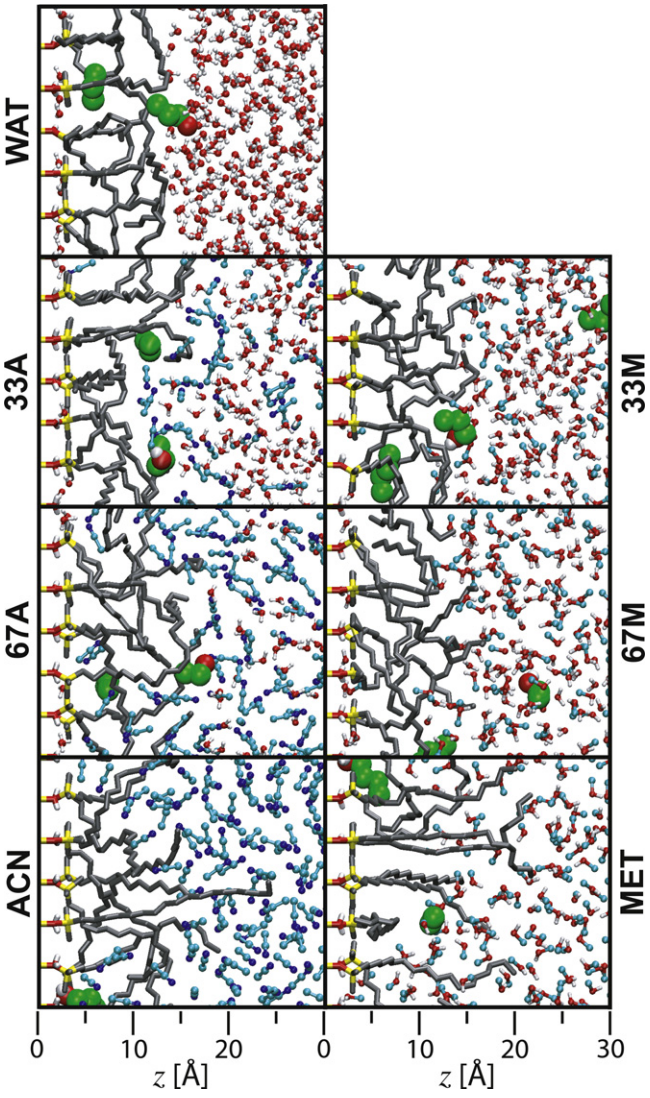

Fig. 1. Simulation snapshots for RPLC systems with varying mobile phase composition. The stationary phase is shown as tubes with carbon in grey, silicon in yellow, and oxygen in red. The mobile phase is shown in the ball and stick representation with carbon in cyan, oxygen in red, nitrogen in blue, and hydrogen in white. Solutes are depicted as large spheres with CH_x units in green, oxygen in red, and hydrogen in white. (For interpretation of the references to color in this figure legend, the reader is referred to the web version of the article.)

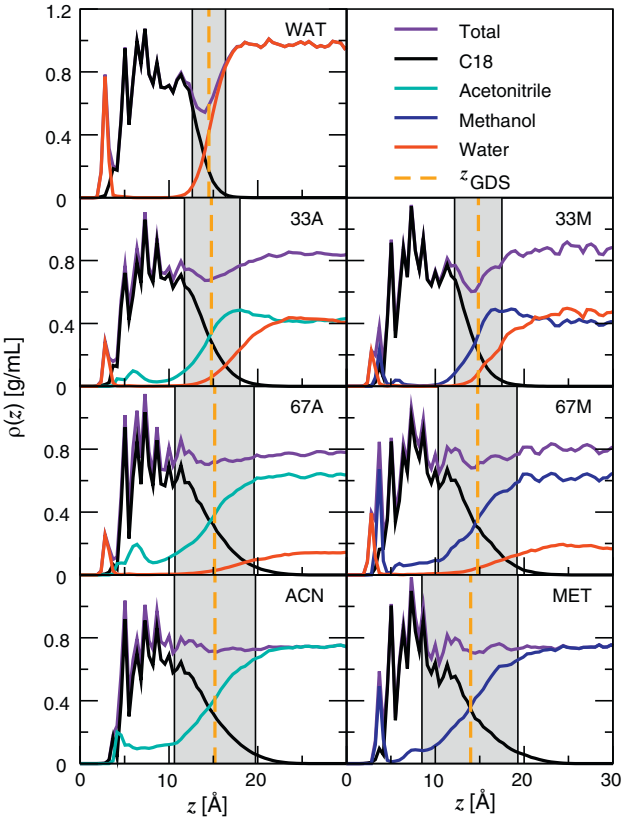

Fig. 2. Solvent and stationary phase density profiles. The shaded gray area represents the interfacial region. Data for systems WAT, 33M, 67M, and MET are taken from [52]. (For interpretation of the references to color in this figure legend, the reader is referred to the web version of the article.)

mobile phases. This is most apparent when viewing the snapshot for system 33A where the region just above the alkyl chains appears to be highly enriched in acetonitrile. The snapshots also indicate that the alkyl chains become more extended and aligned away from the silica surface as the fraction of organic modifier is increased. The solutes present in the snapshots suggest that retention can occur at the surface of the alkyl chains (adsorption) or deep within the bonded phase (partitioning). A full analysis of the simulation trajectory offers more precise details on the preliminary observations from these snapshots. This analysis is the topic of the following subsections.

It should also be noted here that at the bottom of the snapshots shown in Fig. 1 is a scale defining the z-coordinate, which is zero at the silica surface and increases as one moves away from the surface in the z-direction. Many system properties are reported in this paper are given as a function of this z-coordinate. There are two silica surfaces in the model RPLC system utilized here. All properties are reported as averages over these two surfaces.

3.1. Solvation of the stationary phase

To describe the system composition as a function of z, density profiles for the components of the mobile phase and the stationary phase alkyl chains are presented in Fig. 2. Also shown in this figure is the location of the Gibbs dividing surface (GDS), a plane that defines the boundary between mobile and stationary phase [57,83,84], and a shaded area representing the width of this interfacial region. These quantities are fit to the total solvent density (water and organic co-solvent) using a hyperbolic tangent fitting method [85].

In examining the density profiles, one definitely sees an increase in solvent penetration into the chain region as the molfraction of organic modifier is increased. For system WAT, the center of the bonded phase ($z \approx 5$–12 Å) is nearly void of solvent while in systems ACN and MET there is a substantial amount of solvent in this region. For the mixed solvent systems, the solvent component penetrating into the stationary phase is primarily the organic modifier. Despite the increase in solvent penetration with increasing organic molfraction, the location of the GDS does not change significantly and is located at around 15 Å in all systems. However, an increase in the interfacial width is observed with increasing organic molfraction. In system WAT this width is about 4 Å, whereas it is closer to 10 Å in systems ACN and MET. This increase in interfacial width is reflective of both a penetration of solvent into the stationary phase and an extension of the C_{18} chains into the solvent.

In comparing water/acetonitrile and water/methanol mixtures with the same organic molfraction, there is a larger extent of solvent penetration for the acetonitrile containing solvents except very near the silica substrate ($z \approx 4$ Å) where methanol exhibits sharp peaks. These sharp peaks, which are also present in the density

Table 1
Percentage of surface silanols with zero, one, two, or three hydrogen bonds with solvent molecules. [a]

System	0	1	2	3
WAT	21	39	35	4
33A	52	39	9	<1
67A	54	38	7	<1
ACN	85	15	0	0
33M	19	41	36	4
67M	23	43	31	3
MET	33	38	28	1

[a] Uncertainties in all data are less than 2%.

profiles of water, result from solvent molecules directly hydrogen bonding with surface silanols. To quantify this effect, the number of hydrogen bonds between surface silanols and solvent molecules is presented in Table 1. In system WAT, only 21% of silanols are not involved in any hydrogen bonds with solvent molecules and the majority of silanols have either one or two hydrogen bonds with solvent molecules. The number of silanols with no hydrogen bonds increases markedly as acetonitrile concentration is increased. In systems 33A and 67A, the percentage of silanols with no hydrogen bonds is over 50% and in system ACN this number jumps to 85%. For those silanols that are hydrogen bonded to solvent in the acetonitrile containing systems, very few have more the one hydrogen bond. The methanol containing systems are in stark contrast to this. For systems 33M and 67M, the number of silanols with no hydrogen bonds is similar to system WAT and this number increases to only 33% in system MET. In these systems there is also a significant fraction of silanols with two or more hydrogen bonds. The decrease in hydrogen bonding for the acetonitrile containing systems likely stems from the fact that acetonitrile can only be involved in one hydrogen bond (as an acceptor) while methanol can participate in three (donating one and accepting two) and water can participate in four (donating two and accepting two). This lack of hydrogen bonding between surface silanols and solvent molecules in the acetonitrile rich systems has important consequences for the retention of hydrogen bonding solutes, a topic that will be addressed later.

Other interesting phenomenon in the density profiles can be seen in the interfacial region. For system WAT, there is a depletion in the total system density, or partial dewetting near the GDS. This depletion becomes less apparent as the molfraction of organic modifier is increased and disappears in systems ACN and MET. For the mixed solvents, the depletion is stronger for the methanol containing mixtures. This dewetting effect for water near extended hydrophobic surfaces has been predicted by Lum et al. and is attributed to a disruption of the solvent's hydrogen bonding network [86]. It appears that this effect is less important in the more weakly hydrogen bonding acetonitrile mixtures as compared to the methanol mixtures. Also present in the interfacial region is an enrichment in the organic modifier concentration for the binary solvent systems. This effect is most dramatic for systems 33A and 33M where the density of the organic modifier reaches a maximum in the interfacial region, which actually exceeds its bulk mobile phase density. Interestingly, this density maximum occurs near the minimum in total system density. The enrichment in the interfacial region appears to be slightly stronger for the acetonitrile containing systems.

Kazakevich and coworkers have measured the excess adsorption isotherms of acetonitrile and methanol from their mixtures with water onto RPLC stationary phases [27,28]. In this work, they showed that there is a maximum in the excess adsorption of the organic component of the solvent at organic modifier molfractions of around 0.3–0.4, and that the excess adsorption is larger for acetonitrile than for methanol. At this solvent composition, Kazakevich and coworkers inferred that methanol forms one monolayer at the C_{18}/mobile phase interface and acetonitrile forms five molecular layers [28]. In qualitative agreement with this experimental work, it is found here that there is an excess adsorption of the organic component of the solvent and that this excess is greater for acetonitrile mixtures than for methanol mixtures. The excess adsorption can be quantified from the difference between the average number of organic modifier molecules found in the stationary phase box and the average number found in the bulk mobile phase in a volume element equivalent to the volume between the two GDSs in the stationary phase box. From this excess number of organic modifier molecules in the stationary phase box, the cross section of the stationary phase box, and the molar volume of the neat organic phase, we can estimate that the excess adsorption would be equivalent to solvent layers with a thickness of 2.5, 1.9, 0.7 and 0.1 Å for systems 33A, 67A, 33M, and 67M, respectively. In agreement with the experimental data [28], the simulations yield a larger excess adsorption for the solvents with 33% organic modifier compared to those with 67%. For the 33% composition, the excess adsorption would correspond to an organic layer that is about four times thicker for acetonitrile than for methanol.

However, assuming that the adsorption excess relates to a layer of neat organic modifier is not a good representation. The density profiles do show an enhancement of the organic modifier in the interfacial region, but the solvent composition in the interfacial region is never 100% organic modifier and, hence, no distinct layers of organic modifier exist (such layers would be entropically extremely unfavorable). Additionally, since the enhancement of organic modifier in the interfacial region is only slightly greater for the water/acetonitrile mixtures, the increased amount of adsorption of organic modifier for water/acetonitrile as compared to water/methanol mixtures is not solely due to enhancement at the C_{18} surface. Rather, it is also the result of increased partitioning of acetonitrile inside of the C_{18} phase relative to methanol.

Another observation of Kazakevich and coworkers was an excess adsorption of water at very high organic modifier concentrations, i.e., more than 95% (v/v) [28]. This excess water adsorption was attributed to a higher affinity of water to interact with the residual surface silanols as compared to the organic modifier and was observed to be larger for water/acetonitrile mixtures than for water/methanol mixtures. The hydrogen bond data in Table 1 indicates that water does interact more strongly with the surface silanols than either methanol or acetonitrile because, in the neat solvents, water forms more hydrogen bonds with the silanols. Furthermore, this hydrogen bond data can also explain the greater excess of absorbed water in water/acetonitrile mixtures. Neat acetonitrile forms far fewer hydrogen bonds with the silanols than does neat methanol. Thus, in water/acetonitrile mixtures there should be less competition for water molecules to interact with the silica surface.

The orientation of solvent molecules within the stationary phase and interfacial region is also important for characterizing stationary phase solvation. For this reason, the average orientation of end-to-end vectors for acetonitrile and methanol ($\cos\theta_{ete}$) and dipole vectors for water ($\cos\theta_p$) with respect to the substrate normal are plotted as a function of z in Fig. 3. Positive values of $\cos\theta_{ete}$ indicate solvent methyl groups of acetonitrile or methanol pointing towards the silica substrate and negative values indicate methyl groups pointing away. Positive values of $\cos\theta_p$ indicate dipole vectors directed away from the substrate and negative values indicate the opposite orientation.

For acetonitrile there is a definite preference for the methyl group to point away from, and the nitrogen towards, the silica surface for $z < 5$ Å. In this orientation, acetonitrile may interact with the surface silanols via hydrogen bonding. In the region from 5 to 8 Å away from the surface, acetonitrile has a strong preference to orient its methyl group in the opposite direction. Moving outward beyond

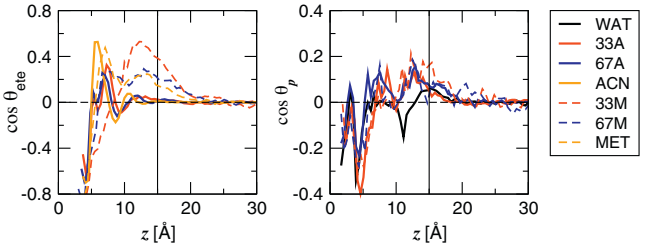

Fig. 3. Orientation of the end-to-end vector of the organic modifier (left) and the dipole vector of water (right) as a function of z. The horizontal line at $z = 15$ Å serves as a rough guide for the position of the GDS in each system. (For interpretation of the references to color in this figure legend, the reader is referred to the web version of the article.)

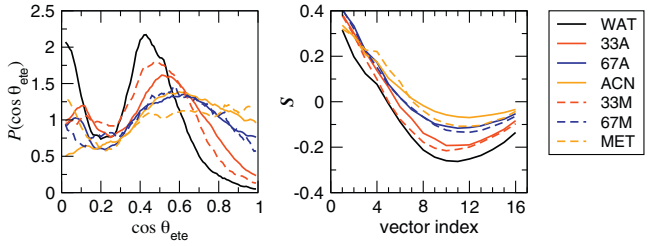

Fig. 4. Probability distribution for the angle between the C_{18} end-to-end vectors and the silica surface normal (left) and the order parameter along the chain backbone (right). Data for systems WAT, 33M, 67M, and MET are taken from [51]. (For interpretation of the references to color in this figure legend, the reader is referred to the web version of the article.)

$z = 8$ Å, $\cos\theta_{ete}$ values for acetonitrile continue to oscillate but soon decay to zero and there is no orientational preference for acetonitrile outside of the GDS. Methanol has an orientational preference similar to acetonitrile when near the silica surface, i.e., it points it methyl group away from and its hydroxyl group towards the surface so that it can hydrogen bond with the surface silanols. In the interfacial region, methanol has a much stronger orientational preference than acetonitrile. Methanol aligns its methyl group towards the stationary phase and its hydroxyl group towards the solvent. In this manner, the hydroxyl group can participate in hydrogen bonding with the mobile phase solvent while the nonpolar methyl group interacts with the alkyl stationary phase. The stronger orientational preference for methanol in the interfacial region, as compared to acetonitrile, is in disagreement with interpretations of spectroscopic data [87] but in agreement with previous molecular dynamics simulations [39]. Water has a somewhat weaker and more rapidly varying orientational preference than acetonitrile or methanol. In general, its dipole vector point towards the silica surface for $z < 5$ Å and towards the mobile phase when in the interfacial region.

3.2. Structure of the stationary phase

From the solvent density profiles shown in Fig. 2, it is clear that the alkyl chains in the stationary phase are solvated to a larger extent when the concentration of organic modifier in the mobile phase is increased and that this solvation is greater for the acetonitrile containing systems. To ascertain what effect this solvation has on the structure of the C_{18} chains in the stationary phase, various structural properties for the alkyl chains were examined (see Table 2 and Fig. 4).

A commonly reported measure of alkyl chain structure is the fraction of gauche defects (f_{gauche}); a small fraction of gauche defects indicates a high degree of chain order. Table 2 lists the fractions of gauche defects, which is very close to 0.26 in all solvent systems. This is in agreement with Raman spectroscopic measurements by Pemberton and coworkers that indicated little dependence of the dihedral angles on solvent composition, especially when compared to the effects of chain surface coverage [29,30].

Also shown in Table 2 is the end-to-end distance (r_{ete}), i.e., the distance between the first methylene group of the chain and the terminal methyl group. This structural parameter also shows little dependence on solvent composition and is around 16 Å in all solvent systems. Interestingly, the fractions of gauche defects and end-to-end distances are very similar to chains in a bulk C_{18} liquid phase [88]. Thus, these structural parameters indicate that the tethered RPLC chains represent a more liquid-like state under these conditions, as opposed to a more ordered solid-like state.

Another important structural characteristic of the RPLC stationary phase is the degree of chain alignment. One parameter to assess this alignment is $\cos\theta_{ete}$, where θ_{ete} is the angle between the chain end-to-end vector and the normal to the silica surface. The average value for $\cos\theta_{ete}$ in each solvent system is shown in Table 2. Unlike the fraction of gauche defects, the orientation of the end-to-end vector changes substantially with changes in solvent composition. In system WAT, the average value of $\cos\theta_{ete}$ is 0.25 and it increases to 0.56 in system ACN and 0.53 in system MET. Thus, the chains are directed more away from the silica surface as organic concentration increases and this effect is slightly greater for acetonitrile containing solvents. A structural parameter complimentary to the end-to-end orientation is z_{CH_3}, the height of the terminal methyl group above the silica surface. As indicated in Table 2, z_{CH_3} also steadily increases as the concentration of organic modifier is increased, thus indicating an extension of the chains into the mobile phase solvent.

In addition to the average value of $\cos\theta_{ete}$, it is useful to examine the distribution of this angle to ascertain if a particular angle is preferred (like the nearly uniform tilt angle observed for alkyl monolayers on metal surfaces [89]). These distributions are shown in Fig. 4. For system WAT, the distribution is clearly bimodal with peaks in $\cos\theta_{ete}$ near values 0 and 0.4, corresponding to chains nearly parallel to the surface and chains with $\theta_{ete} \approx 65^\circ$, respectively. This bimodal behavior also appears in the other solvent systems, but as the concentration of organic modifier is increased the height of the peak corresponding to chains parallel to the surface decreases significantly. Furthermore, the peak corresponding to more extended chains becomes broadened and shifts to around $\cos\theta_{ete} = 0.6$ in the organic-rich systems (67% and 100% organic

Table 2
Structural properties of alkylsilane chains in contact with different mobile phase solvents. [a]

Property	System						
	WAT [51]	33A	67A	ACN	33M [51]	67M [51]	MET [51]
f_{gauche}	0.25_1	0.27_1	0.26_1	0.27_1	0.27_1	0.26_1	0.26_1
r_{ete} (Å)	16.2_3	15.9_3	16.2_4	16.2_2	15.7_3	16.1_3	16.2_3
$\cos\theta_{ete}$	0.25_1	0.46_3	0.52_2	0.56_2	0.43_3	0.51_2	0.53_4
z_{CH_3} (Å)	9.1_1	11.2_3	12.4_1	12.9_3	10.9_1	12.3_1	12.5_4
S_n	-0.14_2	-0.02_1	0.02_2	0.05_1	-0.05_2	0.01_2	0.02_1

[a] Subscripts indicate the statistical uncertainty in the final digit.

modifier). In these systems there is also a significant probability for chains nearly perpendicular to the silica surface ($\cos\theta_{ete}$ close to 1). It is interesting to note that, despite the large differences in end-to-end orientation in the different solvents, there remains a somewhat broad distribution of chain alignments in all systems. There is no single conformation that dominates in any system and there remains a probability for both parallel and perpendicular chains.

Although the end-to-end vector provides a picture of the overall alignment of the chains, more local information on individual segments within the chain can be gleaned by the order parameter S_i along the chain backbone

$$S_i = \frac{1}{2}\langle 3\cos^2\theta_i - 1\rangle \quad (1)$$

where θ_i is the angle between the ith 1–3 backbone vector in the C_{18} chain and the normal to the silica surface. This order parameter is equivalent to the experimentally observable NMR order parameter for deuterated alkyl chains [90,91]. Fig. 4 shows this order parameter for each 1–3 vector along the chain backbone and Table 2 gives S_n, the value of the order parameter averaged over all 16 1–3 backbone vectors.

Like $\cos\theta_{ete}$, S_n indicates that the chains become aligned more perpendicular to the silica surface as the organic modifier concentration is increased. For system WAT, $S_n = -0.14$ indicates a more parallel preference for the 1–3 vectors. The order parameter increases to values slightly greater than zero for systems ACN and MET, indicating 1–3 vectors with a slight perpendicular preference. For comparison, the order parameter would be zero for an isotropic liquid phase and over 0.2 for a liquid-crystalline phase [92].

Looking at the more local information for the order parameter along the chain backbone (Fig. 4), one sees a similar trend for all seven solvent systems. The order parameter is large and positive for the first few backbone vectors and reaches a minimum somewhere near vector number 10. However, the curves are shifted upward as acetonitrile or methanol concentration is increased. Comparing the water/acetonitrile and water/methanol mixtures with the same organic concentration, one sees that curves for water/acetonitrile mixtures are shifted upward by a small amount indicating a slightly greater alignment in these systems.

In comparing the different structural parameters discussed above, it appears that the conformation of the individual chains (as measured through gauche defect fraction and end-to-end length) does not change to a significant extent when the solvent is changed, however, the alignment of the chains is greatly affected. This similarity between gauche defect fractions and end-to-end length has also been observed when comparing isotropic and liquid crystalline-like n-octadecane liquid phases [88]. Thus, it appears that these parameters may not be good for characterizing the degree of order/disorder in an RPLC stationary phase and one should place more emphasis on chain alignment.

Beyond the conformation of the individual chains, another parameter used to described the stationary phase is the bonded phase thickness. One could characterize the bonded phase thickness in multiple ways, for example through the position of the GDS or the height of the terminal methyl group. The current data indicate that the position of the GDS changes very little upon changing solvent composition and is fairly constant at around z = 15 Å. In contrast, the height of the terminal methyl group increases from 9.1 Å in system WAT to 12.9 and 12.5 Å in systems ACN and MET, respectively. Different experimental studies have also sought to characterize this thickness, but these show diverging results. Kazakevich and coworkers found a C_{18} bonded phase thickness of around 9 Å from low-temperature nitrogen adsorption measurements [27] while Sander and coworkers measured a thickness of

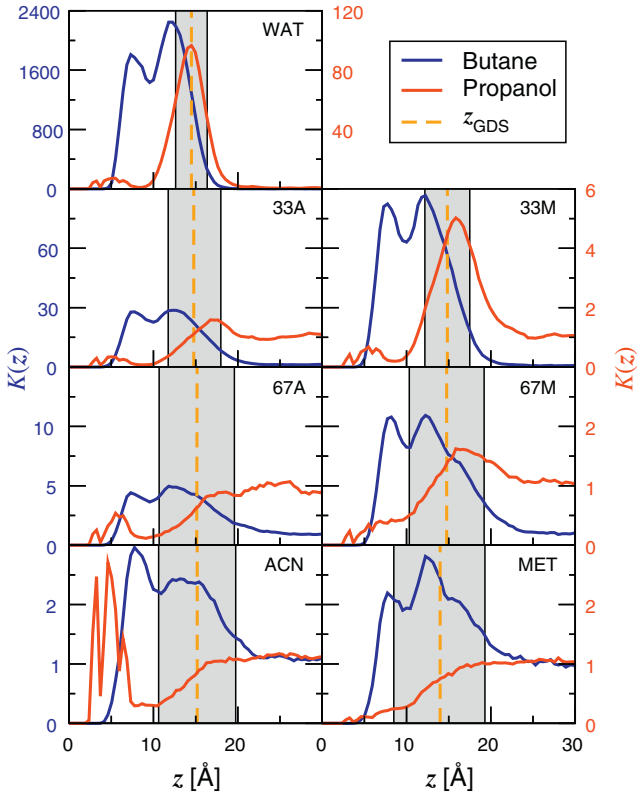

Fig. 5. Distribution coefficient profiles for n-butane and 1-propanol in systems with different mobile phase compositions. Axis scales shown in blue apply to all butane results. Axis scales shown in red apply to all propanol results. Data for systems WAT, 33M, 67M, and MET are taken from [52]. (For interpretation of the references to color in this figure legend, the reader is referred to the web version of the article.)

17±3 Å from neutron scattering experiments for chains in contact with a pure methanol solvent [93]. Assuming low-temperature nitrogen is a poor solvent for the chains, like water, the value of z_{CH_3} seems to agree with the data from Kazakevich and coworkers. However, the value of z_{GDS} is in agreement with the data reported by Sander and coworkers.

3.3. Solute retention

To access the mechanism of solute retention one needs to know, with high resolution, the preferred locations and orientations of the solutes within the stationary phase. The simulations described here are able to directly yield this type of data. The preferred locations of the solutes are described through the z-dependent distribution coefficient profiles, or $K(z)$ plots, shown in Fig. 5 for n-butane and 1-propanol ($K(z) = \rho_{stat}(z)/\rho_{mob}$ where ρ_{mob} is the solute number density in the bulk mobile phase and $\rho_{stat}(z)$ is the z-dependent solute number density in the stationary phase computed for slices with a thickness of 0.45 Å). These profiles are analogous to the (experimentally measurable) distribution coefficient for transfer from mobile to stationary phase but offer much more detailed information on where retention occurs within the stationary phase. That is, larger values of $K(z)$ correspond to more favorable (lower free energy), and thus more rentitive, locations of the solute within the stationary phase. In examining these profiles for all seven systems, one of the most striking features is the large dependence of the solute distribution coefficient on z. With the spatial resolution afforded by the simulations, it is clearly evident that the stationary phase is not a homogeneous medium into which solutes partition nor a nonpolar surface to which solutes adsorb. Rather, the stationary phase is a heterogeneous medium with multiple preferred regions for the solutes.

For butane, the $K(z)$ profiles show a bimodal distribution in all seven solvents. There is one peak in the center of the bonded phase ($z \approx 8$ Å) and another in the interfacial region ($z \approx 12$ Å) but inside the GDS in all systems. The peak in the center of the bonded phase remains rather sharp regardless of solvent composition. However, the shape of the peak in the interfacial region is influenced by solvent composition, broadening as the fraction of organic modifier is increased. The broadening of this interfacial peak coincides with the increasing width of the interfacial region shown in Fig. 2. From this it is apparent that even a simple nonpolar solute has multiple modes of sorption. It can either partition deep into the bonded phase or adsorb at the surface of the hydrocarbon/solvent interface.

The preference of *n*-butane to reside in the interfacial region is not entirely surprising since a density depletion is observed in this region (see Fig. 2) and this would lead to a lower entropic cost of cavity formation. However, the peak deeper in the bonded phase is in a region where the overall system density is significantly higher. Analysis of the bonded-phase structure shows that it is much more ordered in this region, as indicated by the larger S values for the initial portion of the chain (Fig. 4). Thus, there may be more free volume of appropriate size and shape for the solute in this region. The role that chain order may play in retention has recently been reviewed by Sander and co-workers [94]. Free energy minima at the location where the C_{18} density reaches a bulk-like value ($z \approx 13$ Å) and another deeper in the bonded phase were also observed for a methane analyte in molecular dynamics simulations by Klatte and Beck [33], but not by Slusher and Mountain for a C_8 bonded phase [39].

When comparing the water/acetonitrile and water/methanol mixtures with the same organic molfraction, the general shape of butane's $K(z)$ profiles are very similar, but the magnitude of $K(z)$ is larger for the water/methanol mixtures. However, the free energy of transfer from mobile phase to vapor phase is more favorable for butane with water/methanol mixtures than with water/acetonitrile mixtures [58]. This effect was attributed to acetonitriles greater preferential solvation of the methylene group as compared to methanol [58]. Thus, the difference in the magnitude of $K(z)$ stems mainly from the mobile phase contribution and not from changes in the stationary phase. From this it can be concluded that the main features of the retention mechanism of this nonpolar solute do not change for any of the solvent mixtures examined here and remains a mixed partition/adsorption mechanism.

A much different retention mechanism is observed for the polar solute, 1-propanol, and this retention mechanism appears to be somewhat dependent on the mobile phase composition. In system WAT, propanol exhibits a distinct preference to reside in the interfacial region with a peak centered directly on the GDS (but with a peak height much lower than for butane). This preference to adsorb at the alkyl surface clearly diminishes as the fraction of organic modifier is increased and propanol becomes more soluble in the solvent. Additionally, the peak in $K(z)$ shifts to larger z values, from directly under the GDS to the solvent side of the interfacial region as the fraction of organic modifier is increased. This is likely caused by the interfacial enrichment of the organic component of the solvent.

Additional, but smaller peaks in the $K(z)$ profile of propanol are observed in the $3 < z < 7$ Å region of system WAT. These are due to hydrogen bonding of propanol molecules directly to residual surface silanols and to solvent molecules which are bound to the substrate (this is discussed further below). Interestingly these peaks become much stronger as acetonitrile concentration is increased, but not as methanol concentration is increased. This is related to the availability of the surface silanols for hydrogen bonding. In water/methanol mixtures these silanols are nearly saturated by solvent molecules, but in the pure acetonitrile phase the silanols are almost freely available (see Table 1). The presence of hydrogen bonding sites at the silica surface also affects how deeply the alcohol

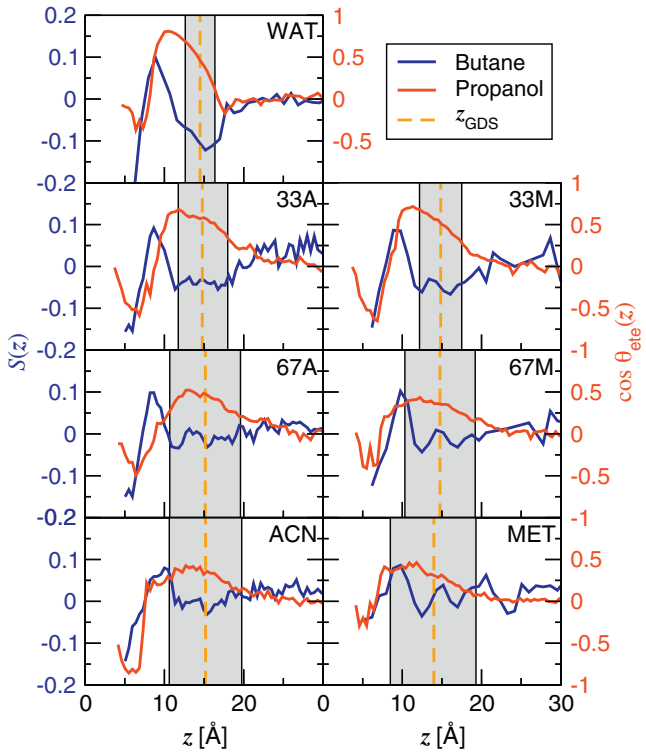

Fig. 6. Order parameter profiles for *n*-butane and end-to-end vector orientation profiles for 1-propanol. Axis scales shown in blue apply to all butane results. Axis scales shown in red apply to all propanol results. Data for systems WAT, 33M, 67M, and MET are taken from [52]. (For interpretation of the references to color in this figure legend, the reader is referred to the web version of the article.)

solute can penetrate into the stationary phase. It is very improbable for the alkane solute to be found at a position with $z \leq 5$ Å, or about where the dimethyl side chains of the $-Si(CH_3)_2C_{18}H_{37}$ alkylsilane groups are located, since this region is very crowded. However, the polar alcohol can exist in this region by partially compensating for the entropic cost of cavity formation through hydrogen bonding to the substrate.

In addition to a comprehension of where a solute is retained within the stationary phase, a complete description of the retention mechanism would also require knowledge of how the solutes are oriented. For this reason, the z-dependent S profiles for butane and $\cos\theta_{ete}$ profiles for propanol are shown in Fig. 6. The end-to-end vector of propanol originates at the methyl group and terminates at the hydroxyl hydrogen. The $S(z)$ profiles for butane show that this solute has some orientational preferences in the stationary phase and interfacial region, although these preferences are quite weak. In the interfacial region, the butane molecule prefers to lie parallel to the interface, seeming consistent with interfacial adsorption. In the center of the bonded phase, butane changes its orientational preference to perpendicular with a maximum in $S(z)$ at around $z = 8$ Å. This maximum occurs at the same position as the peak in the $K(z)$ profile that was attributed to partitioning. Clearly, given the perpendicular orientational preference of butane, this partitioning does not resemble bulk liquid–liquid partitioning where one would see no orientational preference. Moving further into the bonded phase, $S(z)$ values become negative at around $z = 6$ Å, indicating a parallel preference. It appears that the butane solute lies flat as it encounters the "wall" created by the dimethyl side chains. The $S(z)$ profiles for butane look similar in all solvent systems, again suggesting that the retention mechanism is not altered by changes in the organic modifier.

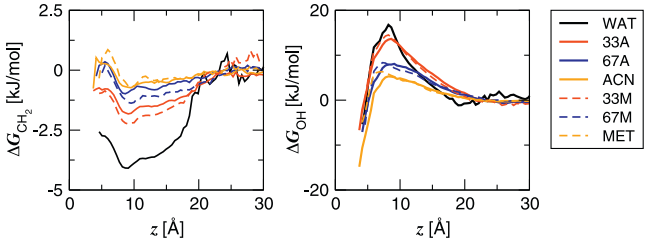

Fig. 7. Incremental retention free energy profiles for the methylene (left) and hydroxyl (right) groups. Data for systems WAT, 33M, 67M, and MET are taken from [52].

Propanol exhibits much stronger orientational preferences than butane. In the interfacial region, the $\cos\theta_{ete}(z)$ profiles indicate that this solute has a preference to direct its hydroxyl group towards the mobile phase and its alkyl tail towards the stationary phase. In this manner the solute can hydrogen bond with the solvent while its nonpolar tail is solvated by the hydrocarbon stationary phase. The magnitude of the interfacial peak in $\cos\theta_{ete}(z)$ decreases as the molfraction of the organic modifier is increased but does not appear to be influenced by whether the organic modifier is acetonitrile or methanol. Moving through the bonded phase to near the silica surface, $\cos\theta_{ete}(z)$ shifts from positive to negative values, thus indicating that the polar hydroxyl group is directed towards the silica surface. In this manner, the propanol solute can form hydrogen bonds with the surface silanols or substrate-bound solvent molecules. This preference is weakest in system WAT, where the silanols are mostly saturated, but very strong in system ACN, where the silanols are mostly unsaturated.

In order to decompose the thermodynamics of retention into contributions from polar and non-polar groups, the incremental free energies of transfer for methylene and hydroxyl groups, ΔG_{CH_2} and ΔG_{OH}, were examined. These two quantities are plotted as a function of z in Fig. 7. $\Delta G_{CH_2}(z)$ is computed by converting the $K(z)$ profiles for ethane, propane, and butane into free energy profiles through the standard relation $\Delta G = -RT\ln K$ [52,57]. A linear regression on the free energy versus number of solute carbons is then performed at each value of z in these profiles. The slope of this regression corresponds to ΔG_{CH_2}. $\Delta G_{OH}(z)$ is found by subtracting the free energy profile for an alkane solute from the free energy profile of an alcohol solute with the same number of carbons.

As can be seen from the profiles, the incremental free energies show a strong dependence on z in the model RPLC system. ΔG_{CH_2} is most favorable at $z \approx 9$ Å, i.e., in the interior of the stationary phase, and its magnitude decreases as the organic molfraction is increased. The general shape of the profile does not depend on whether acetonitrile or methanol is present. However, the profiles for systems 33M and 67M lie slightly below the ones for systems 33A and 67A, whereas the profile for system MET is just above the one for system ACN. These differences are mainly due to the mobile phase contribution to the free energy of retention [58]. In contrast, ΔG_{OH} shows a maximum at $z \approx 9$ Å that is large in magnitude compared to ΔG_{CH_2}. ΔG_{OH} is favorable at $z \approx 5$ Å, where the OH group can hydrogen bond to residual silanols or substrate-bound solvent molecules. ΔG_{OH} is most favorable in system ACN, due to the less favorable mobile phase contribution [58] and enhanced silanol accessibility in this system.

In addition to calculating the incremental free energies of retention as a function of z, they may also be calculated as a net incremental free energy of retention for the entire stationary phase by using the GDS as a border between the mobile and stationary phase and accounting for any excess solute adsorbed at the surface [57]. It should be noted here that the incremental free energy of transfer (or incremental excess chemical potential) will only be strictly constant for a transfer between two homogeneous phases where the homologous series of solutes does not undergo a conformational change as function of chain length [97]. Tchapla et al. [98] have investigated the linearity of retention plots for various homologous solute series in monomeric alkylsilane phases and found a significant discontinuity when the chain lengths of the solute and the stationary phase ligand become comparable and a much smaller change in mean selectivity per methylene segment (corresponding to a change in ΔG_{CH_2} of less than 0.005 kJ/mol) for shorter solute molecules. The probe solutes used in this study are much shorter than the ligands and, hence, should exhibit nearly constant ΔG_{CH_2}. The statistical error in the predicted net values of ΔG_{CH_2} and ΔG_{OH} are <0.1 and <0.5 kJ/mol, respectively. These net incremental free energies of retention are useful because they may be directly compared to experimental retention data. This comparison is made in the free energy level diagram shown in Fig. 8. By assigning the vapor phase as zero on the free energy scale, this diagram also depicts the mobile and stationary phase contributions to the free energy of retention for the realistic model RPLC system described in this work (labeled ODS) and for a liquid n-hexadecane system (labeled C16) described in previous work [58]. Hexadecane is used here to represent what one would expect for bulk liquid–liquid partitioning [7,18]. The experimental retention data in this figure come from careful studies by Barman (for water/methanol mixtures) [95] and Alvarez-Zepeda (for water/acetonitrile mixtures) [96] and for stationary phases very similar to the one modeled here. The experimental data for hexadecane partitioning is from the work of Ranatunga and Carr [23].

First, it is noted that the calculated values of ΔG_{CH_2} are in excellent agreement with experiment (compare the solid and dashed lines above the ODS label in Fig. 8). The largest deviation observed is around 0.2 kJ/mol, a very small value in terms of free energy, and in many cases the deviation is even smaller. Simulation data for the methylene increment in the hexadecane model system also agree very well with experiment, as discussed previously [58]. Reliable retention data for the hydroxyl increment were only available for water/methanol mixtures, but agreement with this data is very good. The fact that the simulations are able to reproduce the thermodynamics of the retention process, as measured experimentally, provides good confidence that the molecular details observed in simulations are indeed correct.

The free energy diagram also allows for a discussion of the driving forces for retention and for a comparison of retention in RPLC to bulk liquid–liquid partitioning. As shown in Fig. 8, the vapor to mobile phase transfer (or mobile phase contribution to retention) for the methylene group is unfavorable only in system WAT. Thus, solvophobic forces [21,99,100] are not important for retention unless highly aqueous mobile phases are used. The free energy of transfer from the vapor phase to the ODS stationary phase (or stationary phase contribution to retention) is always favorable and greater in magnitude than the mobile phase contribution in all solvent systems examined. This is in agreement with the lipophilic view of Carr and coworkers [14,18,23], which argues that interactions with the stationary phase drives the retention process. The free energy of transfer from the vapor phase to the ODS phase changes little with changing solvent composition suggesting that solvent penetration into the stationary phase and its influence on chain order has little effect on nonpolar groups.

Comparing retention in the ODS phase to retention in the hexadecane phase, one sees that they are very similar in terms of free energy. This similarity has been used to suggest that the retention mechanism in RPLC resembles bulk liquid–liquid partitioning [7,18]. The current work shows that this similarity holds only for the integrated $K(z)$ profile but not for specific regions of the stationary phase. The profiles in Figs. 5 and 6 clearly indicate that nonpolar solutes can either partition into the stationary phase or

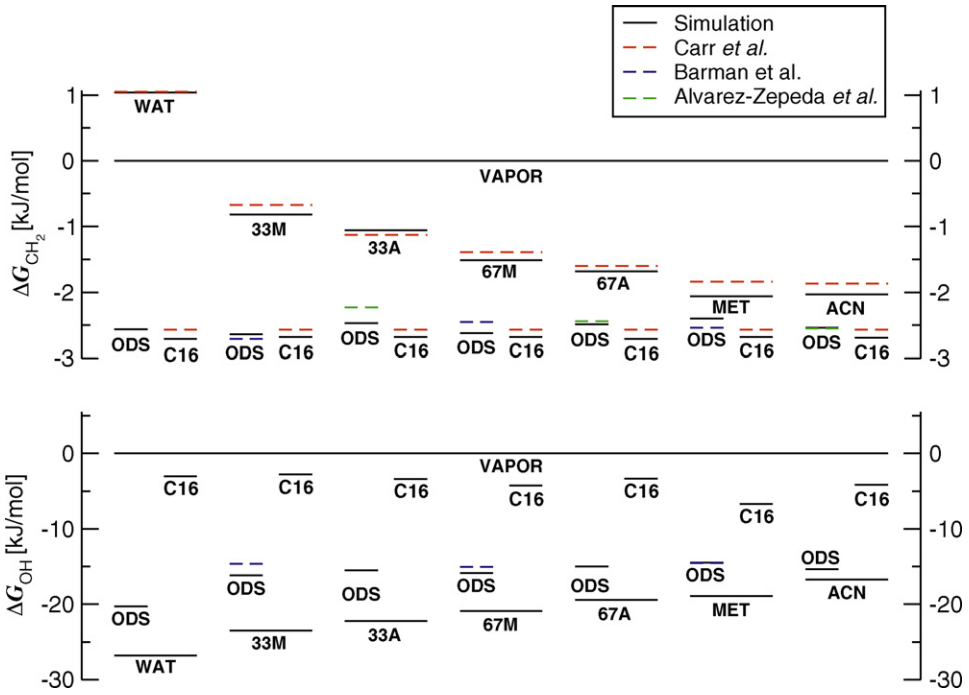

Fig. 8. Incremental free energy level diagrams for the methylene (top) and hydroxyl (bottom) groups. Solid lines indicate values calculated from simulation while dashed lines correspond to experimental values [23,96,95]. Data for ODS and solvents WAT, 33M, 67M, and MET are taken from [52] and data for C16 and all solvents are taken from [58].

adsorb at the surface and in either case have a clear orientational preference, which would not be present in a bulk liquid. Additionally, the free energy of retention for the methylene group in the interfacial region (where adsorption occurs) is slightly smaller, but very similar to the free energy in the center of the bonded phase (where partitioning occurs). Thus, thermodynamics cannot easily distinguish these two processes. This is an excellent example of why great caution should be used when inferring molecular details from thermodynamic data.

For the polar hydroxyl group, the free energy level in the solvent phase is always lower than that in the vapor phase. This indicates an unfavorable transfer from mobile to vapor phase (or mobile phase contribution) and one would view this as a solvophilic, as opposed to a solvophobic force. The magnitude of this solvophilic interaction decreases as the fraction of organic modifier is increased, and is less favorable for the acetonitrile containing solvents. Like for the methylene group, the transfer from the vapor phase to the ODS phase (stationary phase contribution) is favorable, or lipophilic, for the hydroxyl group. However, the magnitude of the solvophilic interaction is much greater.

Comparing the hydroxyl increments for the ODS phase to those for the hexadecane phase, one observes that the former lie significantly lower in free energy than the latter. This effect was observed experimentally by Carr and coworkers for other polar groups [18]. The authors of this work attribute these differences to three possible reasons: (1) hydrogen bonding of polar solutes with the silanols, (2) polar solutes residing at the ODS–mobile phase interface, and (3) polar solutes being preferentially solvated by solvent which is sorbed into the bonded phase [18]. These relative importance of the three items above can be deduced by a hydrogen-bond analysis for the alcohol solutes (see Table 3).

In all seven of the solvent systems, it is found that alcohol solutes, when retained on the stationary phase, hydrogen bond to silanols, sorbed solvent, and solvent outside of the stationary phase. In most of the solvent systems, the prevalent mode of hydrogen bonding is to solvent outside the stationary phase. This is not surprising since interfacial adsorption was the dominant mode of retention in these systems. Hydrogen bonding to surface silanols seems to be the least important contributor, except for system ACN where there is a greater availability of free silanols.

Other trends in the free energy level diagram can be explained by hydrogen bonding. For example, the magnitude of the free energy level in the mobile phase decreases as the fraction of organic modifier is increased. This decrease correlates very well with the decrease in hydrogen bonding in the mobile phase shown in Table 3. It is also interesting to note that an increase in the organic modifier concentration makes the ODS phase less favorable for hydroxyl groups, whereas it makes a bulk hexadecane phase in contact with the same mobile phase more favorable for hydroxyl groups. This is explained by noting that total number of hydrogen bonds in the ODS phase decreases with increasing organic fraction, whereas the

Table 3
Number of hydrogen bonds per alcohol solute molecule in the ODS, mobile, and bulk *n*-hexadecane phases [a,b].

System	N_{SiOH} [c]	N_{in} [d]	N_{out} [e]	N_{total} [f]	N_{mob} [g]	$N_{C_{16}}$ [h]
WAT [52]	0.12_4	0.43_6	1.62_7	2.17_5	2.42_1	0.06_2
33A	0.16_2	0.81_2	0.84_3	1.81_5	1.46_2	0.12_1
67A	0.28_3	0.62_1	0.68_2	1.58_1	1.35_1	0.13_1
ACN	0.82_7	0.28_1	0.27_2	1.37_4	0.66_2	0.18_1
33M [52]	0.08_2	0.41_3	1.48_2	1.97_2	2.17_2	0.30_8
67M [52]	0.09_2	0.57_5	1.24_5	1.90_3	2.01_1	0.9_1
MET [52]	0.07_1	0.41_1	1.34_2	1.82_1	1.83_1	1.33_7

[a] A solute is defined to be in the ODS phase when it is inside the first solvation shell (6 Å) of any stationary phase CH_x segment.
[b] Subscripts indicate the statistical uncertainty in the final digit.
[c] Average number (per alcohol solute molecule) of hydrogen bonds with silanol groups.
[d] Average number of hydrogen bonds with solvent molecules inside the GDS.
[e] Average number of hydrogen bonds with solvent molecules outside the GDS.
[f] Total number of hydrogen bonds in the ODS stationary phase.
[g] Total number of hydrogen bonds in the bulk mobile phase.
[h] Total number of hydrogen bonds in a bulk *n*-hexadecane phase that is in contact with the mobile phase [58].

hexadecane phase shows an increase in hydrogen bonding due to a greater extent of solvent partitioning at higher organic molfractions [58].

4. Conclusions

Simulations of a C_{18} stationary phase in contact with water/acetonitrile and water/methanol mixtures of varying organic modifier concentration indicate that changes in the solvation environment and structure of the stationary phase chains occur with changes in mobile phase composition. As the molfraction of organic modifier is increased, there is a marked increase in the degree of solvent penetration into the bonded phase. Water/acetonitrile mixtures show greater solvent penetration relative to water/methanol mixtures with the same organic molfraction. However, in either case, the primary species partitioned into the bonded phase is the organic modifier. In addition to partitioning into the bonded phase, the solvent is observed to adsorb at the silica surface. This is most important for water and methanol, which interact strongly with the residual surface silanols, saturating nearly all of them. In contrast, acetonitrile has a much weaker interaction with the silica surface. In a pure acetonitrile solvent a very large fraction of the surface silanols would be available for interaction with solute molecules, i.e., peak tailing may be more prevalent.

Interesting phenomena are also observed at the interface between the C_{18} chains and the solvent. In this interfacial region, there is a density depletion, or partial drying effect, especially for solvents with a high molfraction of water. For binary aqueous/organic solvents, there is an enhancement in the concentration of the organic component of the solvent at the interface. This enhancement is only slightly stronger for water/acetonitrile mixtures as compared to water/methanol mixtures.

Ordering of the C_{18} chains in the stationary phase is increased as the concentration of organic modifier is increased. The increased order is seen in parameters that relate to chain alignment ($\cos\theta_{ete}$ and S_n), but parameters that relate to chain conformation (f_{gauche} and r_{ete}) are affected only to a small extent. Interestingly, spectroscopic techniques, such as Raman spectroscopy, typically measure conformational properties like gauche defect fractions. This study shows that parameters related to chain alignment are better indicators of chain ordering.

As far as mobile phase effects are concerned, solvent penetration into the stationary phase appears to be the largest factor contributing to increased chain order. With pure water, there is very little penetration of the solvent and the least amount of chain alignment is observed. In the pure organic solvents, there is a much greater extent of solvent penetration and enhanced chain alignment is seen. In comparing water/acetonitrile and water/methanol mixtures, slightly more penetration of the solvent is observed for the acetonitrile mixtures and this results in a mild increase in chain ordering. However, the differences between water/acetonitrile and water/methanol mixtures with the same organic modifier concentration are much smaller than differences incurred by changing organic modifier concentration. From these results, one can conclude that less polar solvents will penetrate further into the chain structure and produce more chain order. This conclusion is similar to the one reached by Pemberton and coworkers who carried out Raman spectroscopic measurements for a monomeric C_{18} stationary phase at a coverage of 3.09 $\mu mol/m^2$ in contact with a wide range of solvents [29,30].

With regards to the retention mechanism, the most important observation from this simulation study is that the bonded phase does not participate in the retention process as a homogeneous phase. For the alkane solute there clearly exists multiple sorption sites, including the center of the bonded phase and the interfacial region. The existence of sorption site(s) near the interface and the observation that the solute prefers to lie flat in this region suggests that adsorption plays an important role in the retention of this solute. This is in contrast to generally accepted view that the retention of small non-polar solutes is dominated by partitioning [2,7,9,14,15]. The second sorption site for *n*-butane is in the center of the bonded phase, but this region differs from an isotropic alkane phase. Although the molecular-level details are distinctly different, the overall thermodynamics of the RPLC retention process for small nonpolar molecules, as indicated by ΔG_{CH_2}, are similar to bulk oil–water partitioning. The thermodynamic driving force for the retention of the non-polar methylene segment is its *lipophilic* interaction with the bonded phase. This lipophilic interaction is nearly three times larger in magnitude than the unfavorable (or solvophobic) interaction with a neat water mobile phase. Furthermore, the thermodynamic interaction of the methylene segment with water/acetonitrile and water/methanol mobile phases containing 33% or more molfraction organic modifier is favorable, i.e., *solvophilic*. The mechanism of retention for the nonpolar solutes examined here does not exhibit any significant dependence on whether acetonitrile or methanol is used as the organic modifier. Free energies of retention are slightly more favorable in water/methanol mixtures, but this is a mobile phase property and not due to modification of the stationary phase or interfacial region by the mobile phase solvent.

In contrast to *n*-butane, 1-propanol shows a much more distinct preference to reside in the interfacial region and does not partition into the center of the bonded phase. This implies that adsorption in the interfacial region is the most important factor in the retention of this small polar solute. This is in agreement with Martire and Boehm who assert that interfacial adsorption may be of importance for small, polar solutes [2]. In addition to this large contribution from interfacial adsorption, the retention of this alcohol is influenced by its interactions with sorbed solvent molecules and surface silanols. The interaction with surface silanols becomes very important in acetonitrile rich mixtures where the surface silanols are largely unsaturated by solvent molecules. Furthermore, it is observed that the stationary phase in the model RPLC system is drastically different from bulk *n*-hexadecane for the polar solute. The fact that the thermodynamics of RPLC retention for polar solutes may not be well-modeled by *n*-hexadecane partitioning has been suggested previously by Carr and coworkers [14]. Overall, the most important contribution to the distribution of the polar hydroxyl group is its *solvophilic* interaction with the mobile phase that is larger in magnitude than its favorable interaction with the bonded phase.

The data gathered from these simulations provides a new level of insight into the retention process in RPLC. Indeed, some of the commonly held notions about retention have been challenged but it is hoped that the results presented here lead to a more complete understanding of the retention process and improve the field of analytical separation science.

Acknowledgments

Financial support from the National Science Foundation (CHE-0718383) and The Dow Chemical Company is gratefully acknowledged. Part of the computer resources were provided by the Minnesota Supercomputing Institute.

References

[1] H. Colin, G. Guiochon, J. Chromatogr. 158 (1978) 183.
[2] D.E. Martire, R.E. Boehm, J. Phys. Chem. 87 (1983) 1045.
[3] Z. Elkoshi, E. Grushka, J. Phys. Chem. 85 (1981) 2980.
[4] M. Jarionec, D.E. Martire, J. Chromatogr. 351 (1986) 1.
[5] J.A. Marqusee, K.A. Dill, J. Chem. Phys. 96 (1986) 434.
[6] K.A. Dill, J. Phys. Chem. 91 (1987) 1980.

[7] J. Dorsey, K.A. Dill, Chem. Rev. 89 (1989) 331.
[8] P.T. Ying, J.G. Dorsey, K.A. Dill, Anal. Chem. 61 (1989) 2540.
[9] K.B. Sentell, J.G. Dorsey, Anal. Chem. 61 (1989) 930.
[10] K. Sentell, J.G. Dorsey, J. Chromatogr. 461 (1989) 193.
[11] B. Buszewski, Z. Suprynowicz, P. Staszczuk, K. Albert, B. Pfleiderer, E. Bayer, J. Chromatogr. 499 (1990) 305.
[12] P.W. Carr, D.E. Martire, L.R. Snyder, J. Chromatogr. A 656 (1993) 1.
[13] M. Jaroniec, J. Chromatogr. A 656 (1993) 37.
[14] P.W. Carr, J. Li, A.J. Dallas, D.I. Eikens, L.T. Tan, J. Chromatogr. A 656 (1993) 113.
[15] R. Tijssen, P.J. Shoenmakers, M.R. Böhmer, L.K. Koopal, H.A.H. Billiet, J. Chromatogr. A 656 (1993) 135.
[16] L.C. Sander, S.A. Wise, J. Chromatogr. A 656 (1993) 335.
[17] R.E. Boehm, D.E. Martire, J. Phys. Chem. 98 (1994) 1317.
[18] P.W. Carr, L.C. Tan, J.H. Park, J. Chromatogr. A 724 (1996) 1.
[19] J.H. Park, Y.K. Lee, Y.C. Weon, L.C. Tan, J. Li, L. Li, J.F. Evans, P.W. Carr, J. Chromatogr. A 767 (1997) 1.
[20] L.C. Tan, P.W. Carr, J. Chromatogr. A 775 (1997) 1.
[21] A. Vailaya, C. Horváth, J. Chromatogr. A 829 (1998) 1.
[22] D.R. Devido, J.G. Dorsey, H.S. Chan, K.A. Dill, J. Phys. Chem. B 102 (1998) 7272.
[23] R.P.J. Ranatunga, P.W. Carr, Anal. Chem. 72 (2000) 5679.
[24] K. Kaczmarski, W. Prus, T. Kowalska, J. Chromatogr. A 869 (2000) 57.
[25] P. Nikitas, A. Pappa-Louisi, P. Agrafiotou, J. Chromorogr. A 1034 (2004) 41.
[26] F. Gritti, G. Guichon, J. Chromatogr. A 1099 (2005) 1.
[27] I. Rustamov, T. Farcas, F. Chan, R. LoBrutto, H.M. McNair, Y.V. Kazakevich, J. Chromatogr. A 913 (2001) 49.
[28] F. Gritti, Y.V. Kazakevich, G. Guiochon, J. Chromatogr. A 1169 (2007) 111.
[29] J.E. Pemberton, M. Ho, C.J. Orendorff, M.W. Ducey, J. Chromatogr. A 913 (2001) 243.
[30] M.W. Ducey, C.J. Orendorff, J.E. Pemberton, L.C. Sander, Anal. Chem. 74 (2002) 5585.
[31] S.J. Klatte, T.L. Beck, J. Phys. Chem. 97 (1993) 5727.
[32] S.J. Klatte, T.L. Beck, J. Phys. Chem. 99 (1995) 16024.
[33] S.J. Klatte, T.L. Beck, J. Phys. Chem. 100 (1996) 5931.
[34] T.L. Beck, S.J. Klatte, in: J.F. Parcher, T.L. Chester (Eds.), Unified Chromatography, ACS Symposium Series, vol. 748, American Chemical Society, Washington, DC, 2000, p. 67.
[35] M.R. Schure, in: J.J. Pesek, I.E. Leigh (Eds.), Chemically Modified Surfaces, Royal Society of Chemistry, Cambridge, 1994, p. 181.
[36] I. Yarovsky, I. Yu, M.-I. Aguilar, M.T.W. Hearn, J. Chromatogr. A 660 (1994) 75.
[37] I. Yarovsky, M.-I. Aguilar, M.T.W. Hearn, Anal. Chem. 67 (1995) 2145.
[38] I. Yarovsky, M.T.W. Hearn, M.-I. Aguilar, J. Phys. Chem. B 101 (1997) 10962.
[39] J.T. Slusher, R.D. Mountain, J. Phys. Chem. B 103 (1999) 1354.
[40] K.A. Lippa, L.C. Sander, R.D. Mountain, Anal. Chem. 77 (2005) 7852.
[41] K.A. Lippa, L.C. Sander, R.D. Mountain, Anal. Chem. 77 (2005) 7862.
[42] K.A. Lippa, L.C. Sander, J. Chromatogr. A 1128 (2006) 79.
[43] K. Ban, Y. Saito, K. Jinno, Anal. Sci. 20 (2004) 1403.
[44] K. Ban, Y. Saito, K. Jinno, Anal. Sci. 21 (2005) 397.
[45] X. Dou, H. Wang, J. Han, J. Liq. Chromatogr. Relat. Technol. 29 (2006) 2559.
[46] A. Fouqueau, M. Meuwly, R.J. Bemish, J. Phys. Chem. B 111 (2007) 10208.
[47] J. Braun, A. Fouqueau, R.J. Bemish, M. Meuwly, Phys. Chem. Chem. Phys. 10 (2008) 4765.
[48] M. Orzechowski, M. Meuwly, J. Phys. Chem. B 114 (2010) 12203.
[49] S.M. Melnikov, A. Höltzel, A. Seidel-Morgenstern, U. Tallarek, J. Phys. Chem. C 113 (2009) 9230.
[50] L. Zhang, L. Sun, J.I. Siepmann, M.R. Schure, J. Chromatogr. A 1079 (2005) 127.
[51] L. Zhang, J.L. Rafferty, J.I. Siepmann, B. Chen, M.R. Schure, J. Chromatogr. A 1126 (2006) 219.
[52] J.L. Rafferty, L. Zhang, J.I. Siepmann, M.R. Schure, Anal. Chem. 79 (2007) 6551.
[53] J.L. Rafferty, J.I. Siepmann, M.R. Schure, Anal. Chem. 80 (2008) 6214.
[54] J. Rafferty, J. Siepmann, M. Schure, J. Chromatogr. A 1204 (2008) 11.
[55] J. Rafferty, J. Siepmann, M. Schure, J. Chromatogr. A 1204 (2008) 20.
[56] J.L. Rafferty, J.I. Siepmann, M.R. Schure, J. Chromatogr. A 1216 (2008) 2320.
[57] J.L. Rafferty, J.I. Siepmann, M.R. Schure, in: P.R. Brown, E. Grushka (Eds.), Advances in Chromatography, vol. 48, Marcel Dekker, New York, 2010, p. 1.
[58] J.L. Rafferty, L. Sun, J.I. Siepmann, M.R. Schure, Fluid Phase Equilibr. 290 (2010) 25.
[59] J.L. Rafferty, J.I. Siepmann, M.R. Schure, in: B. Kirchner, J. Vrabec (Eds.), Topics in Current Chemistry - Multiscale Molecular Methods in Applied Chemistry, Springer Verlag, Heidelberg, to appear.
[60] P.W. Carr, R.M. Doherty, M.J. Kamlet, R.W. Taft, W. Melander, C. Horváth, Anal. Chem. 58 (1986) 2674.
[61] A.M. Stalcup, D.E. Martire, S.A. Wise, J. Chromatogr. 442 (1988) 1.
[62] A. Alvarez-Zepeda, B.N. Barman, D.E. Martire, Anal. Chem. 64 (1992) 1978.
[63] B.P. Johnson, M.G. Khaledi, J.G. Dorsey, Anal. Chem. 58 (1986) 2354.
[64] J.I. Siepmann, D. Frenkel, Mol. Phys. 75 (1992) 59.
[65] J.I. Siepmann, I.R. McDonald, Mol. Phys 75 (1992) 255.
[66] M.G. Martin, J.I. Siepmann, J. Am. Chem. Soc. 119 (1997) 8921.
[67] M.G. Martin, J.I. Siepmann, J. Phys. Chem. B 103 (1999) 4508.
[68] C.D. Wick, J.I. Siepmann, Marcomolecules 33 (2000) 7207.
[69] A.Z. Panagiotopoulos, N. Quirke, M. Stapleton, D.J. Tildesley, Mol. Phys. 63 (1988) 527.
[70] G.C.A.M. Mooij, D. Frenkel, B. Smit, J. Phys. Condens. Matter 4 (1992) 255.
[71] M.G. Martin, J.I. Siepmann, J. Phys. Chem. B 102 (1998) 2569.
[72] B. Chen, J.J. Potoff, J.I. Siepmann, J. Phys. Chem. B 105 (2001) 3093.
[73] C.D. Wick, J.M. Stubbs, N. Rai, J.I. Siepmann, J. Phys. Chem. B 109 (2005) 18974.
[74] J. Rafferty, L. Zhang, N. Zhuravlev, K. Anderson, B. Eggimann, M. McGrath, Siepmann. J., in: R. Ross, S. Mohanty (Eds.), Large Scale Molecular Dynamics, Nanoscale and Mesoscale Modeling and Simulation, Wiley Publishing, New Jersey, 2008, p. 189.
[75] W.L. Jorgensen, J. Chandrasekhar, J.D. Madura, R.W. Impey, M.L. Klein, J. Chem. Phys. 79 (1983) 926.
[76] A.G. Bezus, A.V. Kiselev, A.A. Lopatkin, P.Q. Du, J. Chem. Soc., Faraday Trans. 74 (1978) 367.
[77] T.J.H. Vlugt, W. Zhu, F. Kapteijn, J.A. Moulijn, B. Smit, R. Krishna, J. Am. Chem. Soc. 120 (1998) 5599.
[78] E. Demiralp, T. Çağin, W.A. Goddard, Phys. Rev. Lett. 82 (1999) 1708.
[79] M.P. Allen, D.J. Tildesley, Computer Simulation of Liquids, Oxford University Press, Oxford, 1987.
[80] R.D. Mountain, J. Phys. Chem. B 114 (2010) 16460.
[81] B. Chen, J.I. Siepmann, J. Am. Chem. Soc. 122 (2000) 6464.
[82] B. Chen, J.I. Siepmann, J. Phys. Chem. B 110 (2006) 3555.
[83] A. Zangwill, Physics at Surfaces, Cambridge University Press, Cambridge, UK, 1988.
[84] A.W. Adamson, A.P. Gast, Physical Chemistry of Surfaces, 6th ed., Wiley-Interscience, New York, 1997.
[85] J.W. Cahn, J.E. Hilliard, J. Chem. Phys. (1958) 258.
[86] K. Lum, D. Chandler, J.D. Weeks, J. Phys. Chem. B 103 (1999) 4570.
[87] M.C. Henry, E.A. Piagessi, J.C. Zesotarski, M.C. Messmer, Langmuir 21 (2005) 6521.
[88] L. Sun, J.I. Siepmann, M.R. Schure, J. Phys. Chem. B 110 (2006) 10519.
[89] J.I. Siepmann, I.R. McDonald, Mol. Phys. 79 (1993) 457.
[90] A. Seelig, J. Seelig, Biochemistry 13 (1974) 4839.
[91] P. van der Ploeg, H.J.C. Berendsen, J. Chem. Phys. 76 (1982) 3271.
[92] P.G. de Gennes, J. Prost, The Physics of Liquid Crystals, 2nd ed., Clarendon Press, Oxford, 1993.
[93] L.C. Sander, C.J. Glinka, S.A. Wise, Anal. Chem. 62 (1990) 1099.
[94] L.C. Sander, K.A. Lippa, S.A. Wise, Anal. Bioanal. Chem. 382 (2008) 646.
[95] B.N. Barman, Ph.D. thesis, Georgetown University, Washington, DC, 1986.
[96] A. Alvarez-Zepeda, Ph.D. thesis, Georgetown University, Washington, DC, 1991.
[97] S.K. Kumar, I. Szleifer, A.Z. Panagiotopoulos, Phys. Rev. Lett. 22 (1991) 2935.
[98] A. Tchapla, H. Colin, G. Guiochon, Anal. Chem. 56 (1984) 621.
[99] C. Horváth, W. Melander, I. Molnár, J. Chromatogr. 125 (1976) 129.
[100] A. Vailaya, C. Horváth, J. Phys. Chem. B 101 (1997) 5875.